© 2014. Published by The Company of Biologists Ltd | The Journal of Experimental Biology (2014) 217, 3346-3355 doi:10.1242/jeb.105825

RESEARCH ARTICLE

Scavenging ROS dramatically increase NMDA receptor whole-cell currents in painted turtle cortical neurons

David James Dukoff[1,*], David William Hogg[1,*], Peter John Hawrysh[1] and Leslie Thomas Buck[1,‡]

ABSTRACT

Oxygen deprivation triggers excitotoxic cell death in mammal neurons through excessive calcium loading via over-activation of *N*-methyl-D-aspartate (NMDA) and alpha-amino-3-hydroxy-5-methyl-4-isoxazolepropionic acid (AMPA) receptors. This does not occur in the western painted turtle, which overwinters for months without oxygen. Neurological damage is avoided through anoxia-mediated decreases in NMDA and AMPA receptor currents that are dependent upon a modest rise in intracellular Ca^{2+} concentrations ($[Ca^{2+}]_i$) originating from mitochondria. Anoxia also blocks mitochondrial reactive oxygen species (ROS) generation, which is another potential signaling mechanism to regulate glutamate receptors. To assess the effects of decreased intracellular [ROS] on NMDA and AMPA receptor currents, we scavenged ROS with *N*-2-mercaptopropionylglycine (MPG) or *N*-acetylcysteine (NAC). Unlike anoxia, ROS scavengers increased NMDA receptor whole-cell currents by 100%, while hydrogen peroxide decreased currents. AMPA receptor currents and $[Ca^{2+}]_i$ concentrations were unaffected by ROS manipulation. Because decreases in [ROS] increased NMDA receptor currents, we next asked whether mitochondrial Ca^{2+} release prevents receptor potentiation during anoxia. Normoxic activation of mitochondrial ATP-sensitive potassium (mK_{ATP}) channels with diazoxide decreased NMDA receptor currents and was unaffected by subsequent ROS scavenging. Diazoxide application following ROS scavenging did not rescue scavenger-mediated increases in NMDA receptor currents. Fluorescent measurement of $[Ca^{2+}]_i$ and ROS levels demonstrated that $[Ca^{2+}]_i$ increases before ROS decreases. We conclude that decreases in ROS concentration are not linked to anoxia-mediated decreases in NMDA/AMPA receptor currents but are rather associated with an increase in NMDA receptor currents that is prevented during anoxia by mitochondrial Ca^{2+} release.

KEY WORDS: Reactive oxidative species, Pyramidal neurons, Whole-cell patch-clamp, Anoxia tolerance, Channel arrest, Calcium, Fluorescence

INTRODUCTION

Aerobic organisms use diatomic oxygen (O_2) as the terminal electron acceptor of the mitochondrial electron transport chain. As a result of inconsistencies in electron flux, a portion of all oxygen consumed (~3%) is left partially reduced as the superoxide anion (Chen et al., 2003; Liu et al., 2002). This highly reactive molecule reacts rapidly with water, leading to the formation of other reactive oxygen species (ROS), the most prevalent and stable of which is hydrogen peroxide (H_2O_2) (Chandel and Schumacker, 2000). Generated ROS diffuse out of the mitochondria and into the intracellular and extracellular environment, where they can oxidize various cellular components (Henzler and Steudle, 2000; Ottaviano et al., 2008). ROS generated from non-mitochondrial sources, including nitric oxide from intracellular nitric oxide synthase and H_2O_2 from extracellular xanthine oxidase, also contribute to baseline ROS concentrations and rates of oxidation (Ottaviano et al., 2008). ROS concentrations are managed by a series of antioxidant proteins including: superoxide dismutase, catalase and glutathione/glutathione peroxidase. This antioxidant defense system maintains intracellular ROS concentrations ($[ROS]_i$) within non-toxic ranges and reverses ROS-mediated protein oxidation (Ottaviano et al., 2008; Sies, 1993). However, despite mechanisms to control changes in ROS levels, significant variations in $[ROS]_i$ and extracellular ROS concentrations can occur (Starkov, 2008). Recently, changes in ROS levels have been identified to play roles in feedback systems and cellular signalling processes through reversible oxidation of critical cysteine residues on target proteins that can alter protein conformation and levels of activity (Cross and Templeton, 2006; D'Autréaux and Toledano, 2007; Rhee et al., 2003).

In the absence of O_2 (anoxia) ROS production ceases and it is not known what effects this may have on cellular metabolism or health. For the most part it is a non-issue as most vertebrate species are unable to survive under anoxic conditions and are deleteriously affected by more than a few minutes of O_2 deprivation. Damage is most rapidly incurred within the central nervous system, where the loss of oxidative phosphorylation reduces ATP production to levels that cannot sustain the high energetic demands of neural tissue. Na^+/K^+-ATPase activity decreases and membrane ion gradients are lost, leading to membrane potential depolarization, increased action potential firing and a rise in excitatory amino acid release. Excessive glutamate release over-activates postsynaptic alpha-amino-3-hydroxy-5-methyl-4-isoxazolepropionic acid (AMPA) receptors, increasing membrane permeability to Na^+ and resulting in membrane potential depolarization and removal of the magnesium (Mg^{2+}) block from the *N*-methyl-D-aspartate (NMDA) receptors. Subsequently, NMDA receptor over-activation results in excessive calcium (Ca^{2+}) influx and eventual excitotoxic cell death (ECD) (Bosley et al., 1983; Choi, 1992). This sequence of events does not occur in the western painted turtle, *Chrysemys picta* Gray 1831. It overwinters at the bottom of ice-covered lakes and ponds for up to 4 months and is naturally anoxia-tolerant (Jackson, 2000; Jackson and Ultsch, 1982). Its ability to withstand extended periods of anoxia is in part due to an increase in inhibitory signaling: in the cerebrocortex, the onset of anoxia results in a large increase in the concentration of the inhibitory neurotransmitter gamma-aminobutyric acid (GABA) (Nilsson and Lutz, 1991). The consequent increase in GABA receptor activity serves to counteract excitatory inputs by effectively 'clamping' the cell near its resting membrane potential, at the reversal potential for the $GABA_A$ receptor (approximately −80 mV). This results in a decrease

[1]Department of Cell and Systems Biology and Department of Ecology and Evolutionary Biology, University of Toronto, Toronto, ON M5S 3G5, Canada.
*These authors contributed equally to this work

‡Author for correspondence (les.buck@utoronto.ca)

Received 24 March 2014; Accepted 24 June 2014

The Journal of Experimental Biology

The Journal of Experimental Biology (2014) doi:10.1242/jeb.105825

List of symbols and abbreviations

aCSF	artificial cerebrospinal fluid
AMPA	alpha-amino-3-hydroxy-5-methyl-4-isoxazolepropionic acid
BAPTA	1,2-bis(o-aminophenoxy)ethane-N,N,N′,N′-tetraacetic acid
$[Ca^{2+}]_i$	intracellular Ca^{2+} concentration
CM-DCF	chloromethyl-2′,7′-dichlorofluorescein
CM-H_2DCF	chloromethyl-2′,7′-dichlorodihydrofluorescein
CM-H_2DCFDA	5-(and-6)-chloromethyl-2′,7′-dichlorodihydrofluorescein diacetate, acetyl ester
ECD	excitotoxic cell death
GABA	gamma-aminobutyric acid
H_2O_2	hydrogen peroxide
mK_{ATP}	mitochondrial ATP-sensitive potassium
MPG	*N*-2-mercaptopropionylglycine
mPTP	mitochondrial permeability transition pore
NAC	*N*-acetylcysteine
NMDA	*N*-methyl-D-aspartate
P_{O_2}	partial pressure of oxygen
R_a	whole-cell access resistance
ROS	reactive oxygen species
$[ROS]_i$	intracellular ROS concentration
Ψ_m	mitochondrial membrane potential

in action potential frequency (75–95%), and a reduction in ATP consumption to a rate met through glycolytic fermentation alone (Pamenter et al., 2011; Pérez-Pinzón et al., 1992).

In the turtle cerebrocortex, pyramidal neurons account for ~80–90% of the neuronal population (Ulinski, 2007). Their response to anoxia is of particular interest because of their glutamatergic nature and their role in ECD in mammals. Anoxia induces a 50% reduction in NMDA- and AMPA-receptor-evoked currents in pyramidal neurons, which protects against excessive receptor activation, Ca^{2+} influx and ECD (Bickler, 1998; Pamenter et al., 2008b; Shin and Buck, 2003). The anoxic downregulation of NMDA and AMPA receptor currents is the result of a mitochondrial-based Ca^{2+} signalling cascade that is initiated by the activation of the mitochondrial ATP-sensitive potassium (mK_{ATP}) channel. Although the mechanism through which anoxia activates mK_{ATP} channels has yet to be established, its activation initiates a decrease in mitochondrial membrane potential (Ψ_m) and triggers subsequent mitochondrial Ca^{2+} release (Hawrysh and Buck, 2013; Pamenter et al., 2008a; Zivkovic and Buck, 2010). The effect of changing [ROS] on NMDA/AMPA receptor activity or $[Ca^{2+}]_i$ in turtle cortical pyramidal neurons has not been explored, although studies in other vertebrate species demonstrate that NMDA receptor activity is significantly increased by a decrease in ROS levels (Aizenman et al., 1989; Bodhinathan et al., 2010; Choi and Lipton, 2000). However, because ROS levels naturally decrease in the anoxic turtle brain, we propose that this will trigger an increase in $[Ca^{2+}]_i$ and a decrease in NMDA and AMPA receptor whole-cell currents (Pamenter et al., 2007). The aims of this study were to determine: (1) whether decreasing $[ROS]_i$ decrease whole-cell evoked NMDA and AMPA receptor currents in turtle pyramidal neurons, (2) whether mitochondrial Ca^{2+} release is induced by ROS scavenging, and (3) using a complex I inhibitor, whether these responses are dependent on mitochondrial ROS production.

RESULTS

Pharmacological ROS scavengers alter $[ROS]_i$

To investigate a role for $[ROS]_i$ in modulating NMDA/AMPA receptor currents, we first confirmed that $[ROS]_i$ were eliminated by our anoxic experimental protocol. Using the chloromethyl derivative of 2′,7′-dichlorodihydrofluorescein diacetate (CM-H_2DCFDA), a ROS-sensitive dye, we measured changes in fluorescence in cortical brain sheets during normoxia and anoxia, and with and without pharmacological ROS modulation. Fluorescence did not change significantly during 1 h of normoxic perfusion (0.46±0.5%; n=8; Fig. 1A,Ci), indicating maintenance of cellular redox homeostasis.

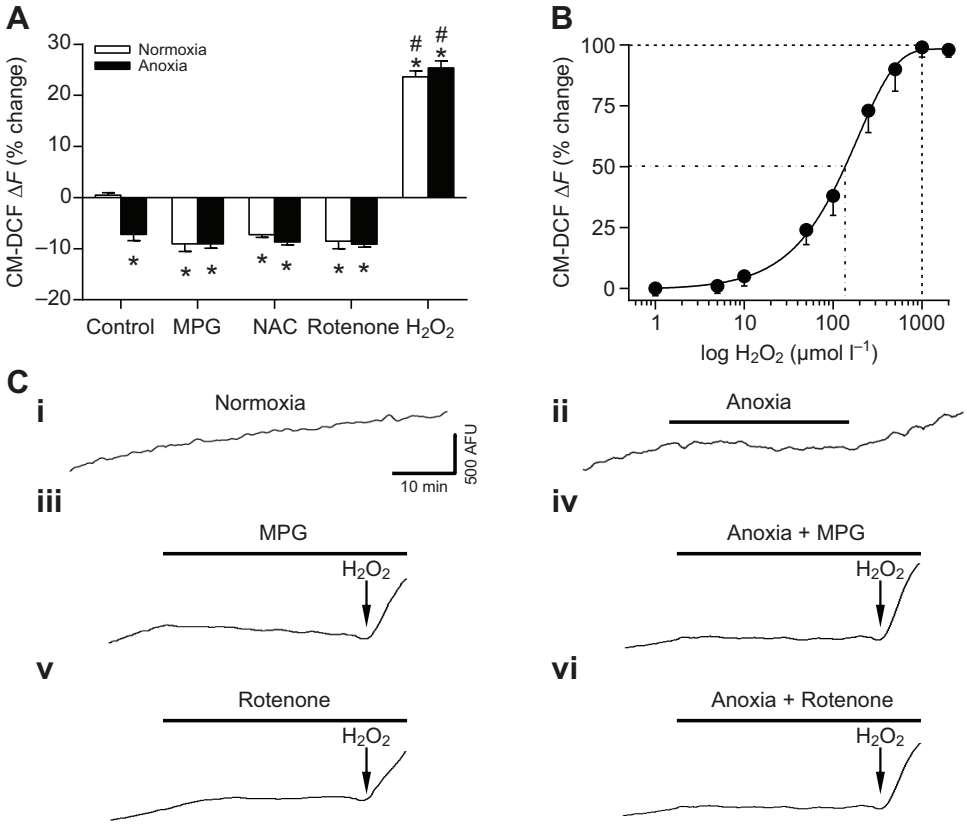

Fig. 1. Anoxia and reactive oxygen species (ROS) scavenging decrease intracellular concentrations of ROS ($[ROS]_i$). (A) Summary of treatment-induced changes in chloromethyl-2′,7′-dichlorofluorescein (CM-DCF) fluorescence (ΔF). (B) Dose–response relationship of $[H_2O_2]$ versus CM-DCF fluorescence. Data in A and B are expressed as means ± s.e.m. *Significant difference from normoxic controls. #Significant difference from anoxic controls (P<0.05). (C) Sample CM-DCF fluorescence recordings from A; neurons treated as indicated. Treatments: (i) normoxia [95% O_2/5% CO_2 bubbled artificial cerebrospinal fluid (aCSF)], (ii) anoxia (95% N_2/5% CO_2 bubbled aCSF), (iii) 0.5 mmol l^{-1} *N*-2-mercaptopropionylglycine (MPG), (iv) anoxia plus 0.5 mmol l^{-1} MPG, (v) 25 μmol l^{-1} rotenone and (vi) anoxia plus 25 μmol l^{-1} rotenone. Black bars represent duration of treatment. Arrows indicate the onset of a 5 min application of 50 μmol l^{-1} H_2O_2 (note: the horizontal linear portion of the trace indicates no new ROS generation). AFU, arbitrary fluorescence units.

The Journal of Experimental Biology (2014) doi:10.1242/jeb.105825

A 30 min anoxic treatment significantly decreased fluorescence (−7.2±1.2%; n=8, P≤0.001; Fig. 1A,Cii) compared with normoxic controls. A 30 min normoxic perfusion with N-2-mercaptopropionylglycine (MPG) or N-acetylcysteine (NAC) (0.5 mmol l^{-1} each) significantly decreased fluorescence (−9.1±1.5 and −7.3±0.5%, respectively; n=5 each, P≤0.001 for both; Fig. 1A,Ciii) compared with normoxic controls. Conversely, the addition of MPG or NAC during anoxia did not significantly decrease fluorescence beyond the effects of either anoxia alone or normoxia plus ROS scavengers (−9.2±0.9 and −8.7±0.5%, respectively; n=5 each; Fig. 1Ciii,iv). The mitochondrial electron transport chain is the primary source of ROS generation in the cell, making it a potentially important component of any ROS-mediated signaling cascade. To investigate the connection between decreased mitochondrial ROS production and NMDA/AMPA receptor function, we added rotenone (25 µmol l^{-1}), a complex I (NADH dehydrogenase) inhibitor, to the perfusate. A 30 min perfusion of normoxic artificial cerebrospinal fluid (aCSF) plus rotenone significantly decreased CM-DCF fluorescence by −8.6±1.5% (n=4, P≤0.001; Fig. 1A,Cv), while addition of rotenone during anoxia had no additional effect (−9.1±0.6%; n=4; Fig. 1A,Cvi). To demonstrate that ROS levels could be experimentally increased, we used H_2O_2 and first determined an appropriate physiological concentration of H_2O_2 to apply. Drip application of H_2O_2 increased CM-DCF fluorescence in a dose-dependent manner (n=4–8 each; Fig. 1B), with 50 µmol l^{-1} [H_2O_2] being the lowest concentration at which we could detect a significant change in fluorescence. This finding is in agreement with normoxic measurements of H_2O_2 from the media of cultured turtle neurons and is near the reported physiological range of mammalian neuronal $[H_2O_2]_i$ (1–20 µmol l^{-1}) (Hoyt et al., 1997; Lei et al., 1998; Milton et al., 2007). In addition, this concentration did not affect baseline electrophysiological properties of pyramidal neurons, such as membrane potential, whole-cell conductance and action potential threshold, indicating that it did not induce oxidative damage (Table 1). A 5 min application of H_2O_2 significantly increased fluorescence during both normoxia and anoxia (23.6±1.1 and 25.4±1.3%, respectively; n=5 each, P≤0.001 for both; Fig. 1A).

Pharmacological ROS manipulation modifies NMDA receptor activity

Evoked NMDA receptor current amplitudes did not change significantly after 90 min of normoxic perfusion (n=8 each; Fig. 2A,Bi). Anoxic perfusion decreased evoked NMDA receptor currents after 20 (61.9±8.6%; n=7, P=0.004) and 40 min (58.6±9.0%; n=7, P=0.008) of treatment, and were reversed after 20 (82.7±12.2%; n=6) and 40 min (98.2±4.2%; n=5) of normoxic washout (Fig. 2A,Bii). (Note: 20 and 40 min treatment values were not significantly different; therefore, only the 20 min data are presented in summary graphs.) ROS scavenging during normoxia increased evoked NMDA receptor currents after 20 (201.4±7.1%; n=6, P=0.001) and 40 min (195.1±16.3%; n=4, P≤0.001) of MPG application (Fig. 2A,Biii) or after 20 (192.5±19.9%; n=6, P=0.046) and 40 min (208.9±37.3%; n=4, P=0.035) of NAC application (Fig. 2A,Biv). The effects of these increases resulted in hyperactivity, depolarization in all patches and the loss of the patch in ~50% of recordings. In situations where the patch was maintained, normoxic washout failed to reverse the effects of MPG after 20 and 40 min (182.8±16.3 and 186.7±5.3%, respectively; n=3 each, P<0.001 for both) but a trend towards recovery was observed

Table 1. Effect of 50 µmol l^{-1} H_2O_2 on electrophysiological parameters of cortical pyramidal neurons in the western painted turtle

	Normoxia	H_2O_2
Membrane potential (mV)	−86.3±0.6	−80.3±3.1
Whole-cell conductance (nS)	4.3±0.6	4.4±0.5
Action potential threshold (mV)	−43.5±1.4	−39.3±1.2

Data shown represent means ± s.e.m. (n=4 per treatment). A t-test comparing normoxia with H_2O_2 within each measured parameter normoxic found the data to not be significantly different.

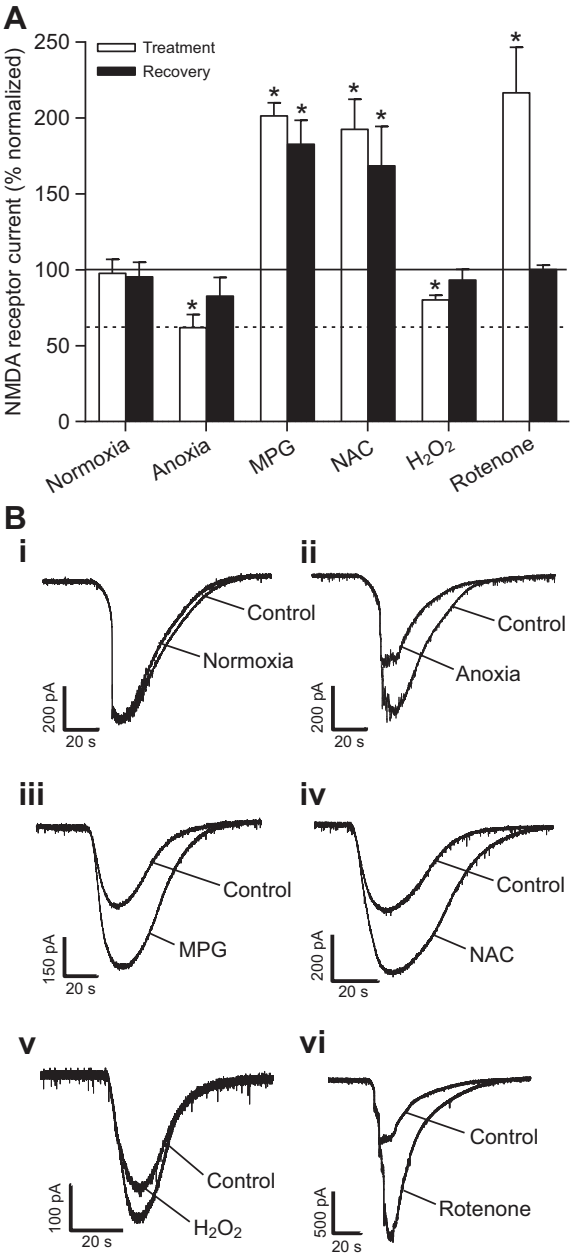

Fig. 2. *N*-methyl-D-aspartate (NMDA) receptor currents are modulated by ROS. (A) Whole-cell NMDA receptor peak current amplitudes following 20 min of treatment and 20 min of washout. Continuous line represents normoxic controls; dashed line represents anoxic controls. Data are expressed as means ± s.e.m. *Significant difference from the paired normoxic control (P<0.05). (B) Sample paired NMDA receptor current recordings of the normoxic baseline current and following 20 min of the indicated treatment (i–vi). The 20 and 40 min treatment and recovery values did not differ statistically; therefore, only the 20 min data have been included.

The Journal of Experimental Biology (2014) doi:10.1242/jeb.105825

after 20 and 40 min of NAC washout (168.4±26.1 and 139.6±24.7%; n=3 each; Fig. 2A). H_2O_2 addition during normoxia decreased evoked NMDA receptor currents after 20 (80.2±3.1%; n=9, P=0.023) and 40 min (78.4±4.4%; n=5; P=0.036) of treatment, which was reversed after 20 and 40 min of normoxic washout (93.2±7.1 and 99.3±7.8%, respectively; n=4 each; Fig. 2A,Bv).

Inhibition of mitochondrial ROS production increases NMDA receptor currents

In order to evaluate the role of mitochondrial produced ROS in regulation of NMDA receptor activity, the complex I inhibitor rotenone was administered under normoxic conditions to prevent mitochondrial ROS formation. Rotenone increased evoked NMDA receptor currents after 20 (216.6±30.1%; n=5, P=0.017) and 40 min (232.3±28.5%; n=4, P=0.01) of treatment, which was reversed after 20 and 40 min of normoxic washout (100.1±2.9 and 104.6±3.4%, respectively; n=3 each; Fig. 2A,Bvi). To determine that this was not a result of the chloroform used to solubilise rotenone, neurons were exposed to a saline solution containing 0.05% chloroform and this did not affect NMDA receptor currents after 20 (106.9±3.9%; n=3) or 40 min (109.5±0.18%; n=3) of treatment (data not shown).

Pharmacological ROS manipulation does not modify AMPA receptor activity

Evoked AMPA receptor current amplitudes did not change significantly after 90 min of normoxic perfusions (n=6 each; Fig. 3A,Bi). Anoxic perfusion decreased evoked AMPA receptor currents at 20 (69.95±5.69%; n=5, P=0.006) and 40 min (55.16±6.04%; n=5, P=0.001), and were reversed after 20 and 40 min of normoxic washout (98.8±4.9 and 101.3±5.2%; n=4 each; Fig. 3A,Bii). (Note: 20 and 40 min treatment values were not significantly different; therefore, only the 20 min data are presented in summary graphs.) ROS scavenging during normoxia had no effect on evoked AMPA receptor currents after 20 (105.4±4.6%; n=6) and 40 min (94.7±7.3%; n=4) of MPG application (Fig. 3A,Biii) or after 20 (100.5±3.2%; n=7) and 40 min (103.5±2.8%; n=6) of NAC application (Fig. 3A,Biv). Currents remained unchanged through 20 and 40 min of normoxic washout following MPG (95.26±3.29 and 97.81±12.60%, respectively; n=4 and 3, respectively) and NAC applications (98.62±2.81 and 97.04±3.86%, respectively; n=4 and 3, respectively; Fig. 3A). H_2O_2 addition during normoxia had no effect on evoked AMPA receptor currents after 20 (100.0±3.4%; n=11) and 40 min (99.2±2.4%; n=7) of treatment, and remained unchanged through 20 and 40 min of normoxic washout (106.33±3.91 and 100.00±2.95%, respectively; n=5 and 3, respectively; Fig. 3A,Bv).

Pharmacological ROS manipulation has no effect on $[Ca^{2+}]_i$

To investigate whether $[ROS]_i$ modulates Ca^{2+} signalling, we next assessed the effect of pharmacological ROS scavenging on $[Ca^{2+}]_i$. Using the Ca^{2+}-sensitive dye Oregon Green, we measured changes in fluorescence in cortical brain sheets with and without pharmacological ROS modulation. Fluorescence did not change significantly from baseline following 20 min of normoxic perfusion (0.6±0.8%; n=6; Fig. 4A,Bi). Anoxic perfusion resulted in a significant increase in fluorescence (16.9±3.3%; n=6, P=0.001; Fig. 4A,Bii) while ROS scavenging with MPG (0.6±0.6%; n=6; Fig. 4A,Biii) or NAC (1.0±1.3%; n=6; Fig. 4A,Biv) or addition of H_2O_2 (0.84±1.39%; n=6; Fig. 4A,Bv) did not significantly change fluorescence.

Exposure to MPG or NAC beyond the 40 min treatment period resulted in a slow increase in fluorescence (11.4±0.9% over 10 min; n=4; data not shown). Drip perfusion of APV [(2R)-amino-5-phosphonovaleric acid, a selective NMDA receptor inhibitor] reduced the fluorescent increase (5.1±0.5% over 10 min; n=4; data not shown), indicating that Ca^{2+} influx through NMDA receptors is likely the source of this increase. This supports our findings that (1) long-term ROS scavenger perfusion is toxic to neurons because of over-activation of NMDA receptors and (2) that ROS-scavenger-

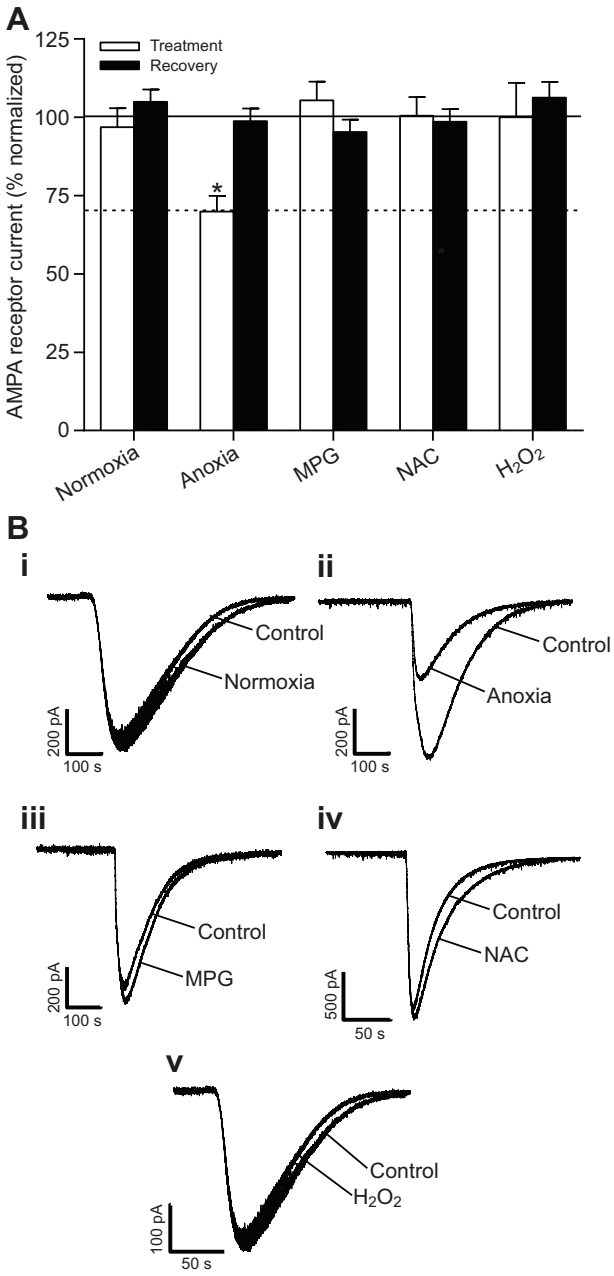

Fig. 3. Alpha-amino-3-hydroxy-5-methyl-4-isoxazolepropionic acid (AMPA) receptor currents are unaffected by pharmacological ROS manipulation. (A) Whole-cell AMPA receptor peak current amplitudes after 20 min of treatment and 20 min of washout. Continuous line represents normoxic controls, dashed line represents anoxic controls. Data are expressed as means ± s.e.m. *Significant difference from the paired normoxic control (P<0.05). (B) Paired sample AMPA receptor current recordings of the normoxic baseline and following 20 min of the indicated treatment (i–v). The 20 and 40 min treatment and recovery values did not differ statistically; therefore, only the 20 min data have been included.

The Journal of Experimental Biology (2014) doi:10.1242/jeb.105825

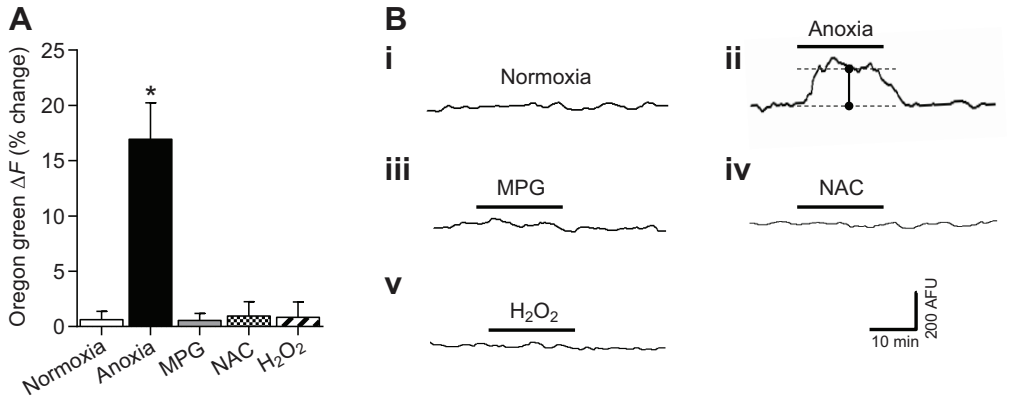

Fig. 4. Manipulation of $[ROS]_i$ has no effect on $[Ca^{2+}]_i$. (A) Summary of treatment-induced changes in Oregon Green fluorescence. Data are expressed as means ± s.e.m. *Significant difference from the paired normoxic control (P<0.001). (B) Drift-corrected sample traces from A; neurons treated as indicated (i–v). Black bars represent duration of treatment. Changes in fluorescence were calculated between two steady-state parallel tangents, as illustrated in Bii.

treated neurons are difficult to recover. Because there is a ROS-scavenger-mediated increase in Ca^{2+}, it is possible that data collected at the 40 min time point could be modulated by Ca^{2+}-activated signaling proteins. However, because experiments were completed prior to the ROS-scavenger-mediated increase in $[Ca^{2+}]_i$, it is not likely that this was a factor. This is supported by whole-cell patch clamp experiments where inclusion of 1,2-bis(o-aminophenoxy) ethane-N,N,N′,N′-tetraacetic acid (BAPTA) in the pipette (5 mmol l^{-1}) did not prevent MPG-mediated increases in NMDA receptor currents after 20 (205.37±23.58%; n=4, P=0.020) or 40 min (222.65±33.24%; n=4, P=0.012; data not shown).

Anoxia-mediated changes in NMDA receptor activity are unaffected by H_2O_2 application

To determine whether anoxic downregulation of NMDA receptor current amplitudes were affected by increases in ROS, H_2O_2 was applied following the transition to anoxia and changes in NMDA receptor currents were measured. Anoxic perfusion alone decreased evoked NMDA receptor currents after 20 (69.6±3.5%; n=5, P=0.031) and 40 min (66.6±6.0%; n=5, P=0.013) of treatment. Subsequent anoxic H_2O_2 administration did not reverse the decrease in NMDA receptor current amplitudes after 20 (58.6±6.73%; n=5, P=0.001) and 40 min (54.36±5.57%; n=5, P<0.001) of treatment; changes were not significantly different from anoxia alone (P>0.05). Normoxic washout did not reverse the anoxic effects after 20 min (59.00±11.48%; n=3, P=0.005) but did reverse them after 40 min (75.36±10.10%; n=3; Fig. 5).

Mitochondrial Ca^{2+} release prevents ROS-scavenger-induced increases in NMDA receptor currents

Anoxia-mediated activation of mK_{ATP} channels leads to mitochondrial Ca^{2+} release and prevents excessive NMDA receptor currents (Hawrysh and Buck, 2013; Pamenter et al., 2008a; Zivkovic and Buck, 2010). However, this occurs at the same time as decreasing $[ROS]_i$, which we found to increase NMDA receptor currents. To better understand the interaction of anoxic mitochondrial Ca^{2+} release and decreasing $[ROS]_i$ on NMDA receptor currents, we pharmacologically modulated both signals and assessed the effect on whole-cell NMDA receptor currents. First, we tested the effect of pharmacologically increasing mitochondrial Ca^{2+} release prior to ROS scavenging. To achieve a small increase in $[Ca^{2+}]_i$ and generate reductions in NMDA receptor currents, the mK_{ATP} channel activator diazoxide was administered (Pamenter et al., 2008a; Zivkovic and Buck, 2010). Diazoxide administration decreased evoked NMDA receptor currents after 20 (66.9±3.9%; n=5, P=0.049) and 40 min (62.6±5.7%; n=5, P=0.022) of treatment (Fig. 5A,Bii). MPG application following diazoxide treatment did not produce increases in NMDA receptor current amplitudes after 20 (57.3±5.5%; n=5, P=0.008) and 40 min (62.8±8.8%; n=4, P=0.036) or produce changes significantly different from diazoxide alone (P>0.05; Fig. 5A,Bii). The effects were reversed after 20 and 40 min of normoxic washout (83.7±21.2 and 89.8±22.6%, respectively; n=4 each; Fig. 5A,Bii). To determine whether the effects of ROS scavenging are reversed by an increase in $[Ca^{2+}]_i$, diazoxide was applied after the addition of MPG. MPG application was limited to 20 min in order to try and prevent the loss of patch encountered in previous ROS scavenging experiments and attributed to NMDA receptor over-activation. MPG administration increased evoked NMDA receptor currents after 20 min (198.9±21.2%; n=4, P=0.001; Fig. 5A,D). Subsequent diazoxide application did not reverse MPG effects significantly after 20 (180.4±11.8%; n=4, P=0.003) or 40 min (175.4±19.8%; n=4, P=0.006; Fig. 5A,Biii). The effects were reversed after 20 and 40 min of normoxic washout (101.6±11.4 and 104.2±8.0%, respectively; n=4 each; Fig. 5A).

Increases in $[Ca^{2+}]_i$ and decreases in Ψ_m occur prior to $[ROS]_i$ decreases during anoxia

To understand the sequence of events leading to anoxic NMDA and AMPA receptor inhibition, we next assessed the timeline of changes in partial pressure of oxygen ($\dot{P}_{O_2}$), Ψ_m, $[Ca^{2+}]_i$ and $[ROS]_i$. First, we assessed the changes in bath chamber $\dot{P}_{O_2}$ using a fluorescent O_2 probe placed in the center of the bath chamber during a 30 min anoxic perfusion and recovery. Bath chamber $\dot{P}_{O_2}$ significantly decreased from a normoxic value of 147.32±2.8 mmHg to 0.52±0.3 mmHg during a 30 min anoxic treatment (n=5, P≤0.001; Fig. 6A). Reperfusion with normoxic aCSF returned chamber $\dot{P}_{O_2}$ levels to the pre-anoxic values (146.4±2.7 mmHg; n=5). Following the switch to anoxic perfusion, the onset of the decrease in chamber $\dot{P}_{O_2}$ occurred in 6.0±0.7 s and reached a steady-state level by 607±63.7 s (n=5 each). The Ca^{2+} signal responsible for modulating NMDA and AMPA receptor currents during anoxia originates from the mitochondria and is the result of depolarization of Ψ_m. To investigate the timeline of this Ca^{2+} signal, we assessed the onset and steady-state changes in Ψ_m using the fluorescent dye rhodamine-123 and changes in $[Ca^{2+}]_i$ with Oregon Green. The onset of the increase in rhodamine fluorescence (Ψ_m depolarization) occurred 70.6±5.1 s after the switch to anoxia and reached a steady state 355±25.1 s after the switch (n=11 each; Fig. 6B). The onset of Oregon Green fluorescence increase (elevated $[Ca^{2+}]_i$) began 70.4±5.6 s after the switch to anoxia and reached steady state 196±19.9 s after the switch to anoxia (n=5 for each; Fig. 6C). The rate of ROS generation started to decrease 120.2±7.6 s after the anoxic switch and reached a plateau indicating no new ROS formation 597±62.8 s after the anoxic switch (n=8 each; Fig. 6D).

The Journal of Experimental Biology (2014) doi:10.1242/jeb.105825

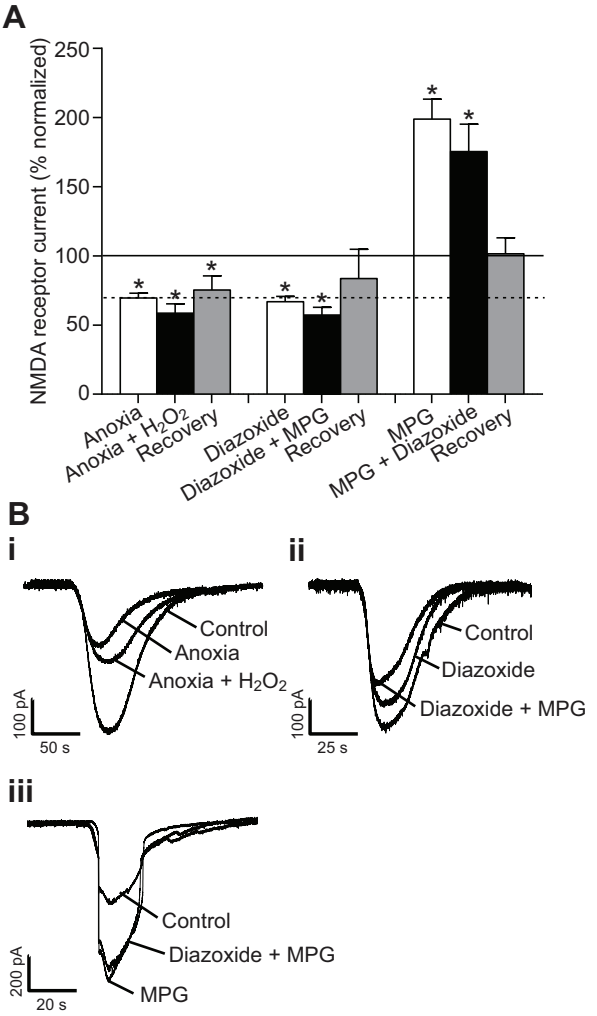

Fig. 5. Anoxia- or mitochondrial-Ca^{2+}-release-mediated NMDA receptor changes are unaffected by ROS manipulation. (A) Whole-cell NMDA receptor peak current amplitudes after 20 min of treatment 1, 20 min of combination treatment 2, and 20 min of washout. Continuous line represents normoxic controls; dashed line represents anoxic controls. Data are expressed as means ± s.e.m. *Significant difference from the paired normoxic control (P<0.05). (B) Paired sample whole-cell NMDA receptor current recordings of the normoxic baseline, following 20 min of the indicated initial treatment and after 20 min of the indicated combination treatment (i–iii). The 20 and 40 min treatment and recovery values did not differ statistically; therefore, only the 20 min data have been included.

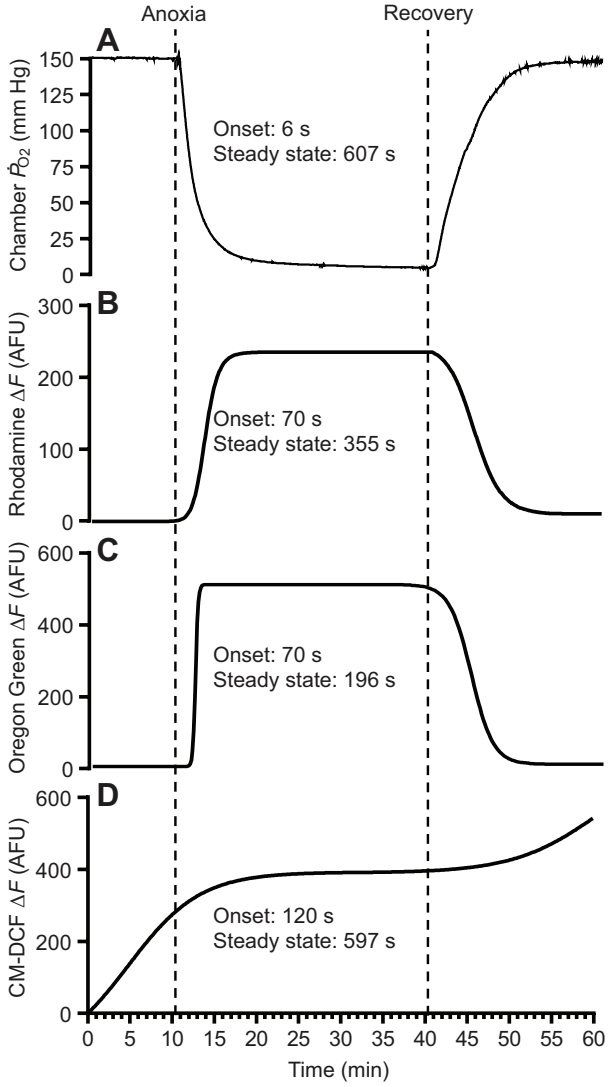

Fig. 6. Timeline of anoxia-induced changes in partial pressure of oxygen ($\dot{P}_{O_2}$), mitochondrial membrane potential (Ψ_m), $[Ca^{2+}]_i$ and $[ROS]_i$. (A) Sample trace of bath chamber $\dot{P}_{O_2}$ during anoxic treatment protocol. (B) Rhodamine fluorescence trace demonstrating the timing of Ψ_m depolarization with anoxic treatment (n=11). (C) Oregon Green fluorescence trace showing changes in $[Ca^{2+}]_i$ with anoxia (n=5). (D) CM-H_2DCF trace outlining changes in $[ROS]_i$ with anoxia (n=8). Time to the onset of the response following the switch to anoxic perfusion and the time to steady-state levels are shown in each panel. Each trace in B–D represents an average of 10 regions of interest per replicate. The onset and recovery portions of the traces were fitted with a non-linear four-parameter curve to reduce noise and highlight the timeline of events. Data in B and C were drift corrected and data in B–D were artificially set to a baseline fluorescence of zero to simplify interpretation of the figure.

DISCUSSION

In this study we explored the effects of scavenging ROS on glutamatergic signalling in pyramidal neurons of the anoxia-tolerant western painted turtle. To our knowledge this is the first investigation into the effects of oxidizing/reducing agents on glutamate receptor activity in reptiles. Using pharmacological ROS scavengers, we demonstrate that decreases in $[ROS]_i$ do not initiate an increase in $[Ca^{2+}]_i$ or reductions in NMDA and AMPA receptor currents during anoxia (Pamenter et al., 2008b; Zivkovic and Buck, 2010). Under normoxic conditions, the application of ROS scavenging agents (MPG or NAC) or H_2O_2 did not have an effect on $[Ca^{2+}]_i$ or AMPA receptor whole-cell currents (Figs 3, 4). The application of ROS scavenging agents resulted in an approximately 100% increase in NMDA receptor whole-cell currents while exogenous application of H_2O_2 decreased whole-cell currents by approximately 20% (Fig. 2). Furthermore, the re-introduction of ROS via H_2O_2 application under anoxic conditions did not reverse anoxia-mediated decreases in NMDA receptor currents.

Our findings of a change in NMDA receptor currents and no effect on AMPA receptor currents in response to ROS scavenging is consistent with results from studies of other vertebrate species in which application of oxidizing agents (e.g. 5,5′-dithiobis-2-nitrobenzoic acid or glutathione disulfide) decrease and reducing agents (e.g. dithiothreitol) increase NMDA receptor currents and neither treatment affects AMPA receptor currents (Aizenman et al.,

1989; Bodhinathan et al., 2010; Choi et al., 2001; Choi and Lipton, 2000; Gozlan et al., 1995; Janáky et al., 1993). The increase in NMDA receptor currents resulting from application of reducing agents is generally six to 11 times greater than decreases initiated by oxidizing agents, a ratio comparable to the 5:1 we found for ROS scavenging or H_2O_2 application in turtle pyramidal neurons (Aizenman et al., 1989; Bodhinathan et al., 2010; Choi and Lipton, 2000). The large increase in receptor currents triggered by ROS scavenging may permit excessive Ca^{2+} influx into patched pyramidal cells during NMDA application, explaining why NAC/MPG application often resulted in cell depolarization and death. The redox sensitivity of NMDA receptors has been attributed to the existence of extracellular cysteine residues located on specific NMDA receptor subunits (GluN1, GluN2A and GluN2B), collectively termed NMDA receptor redox modulatory sites (Choi et al., 2001; Gozlan and Ben-Ari, 1995; Kim et al., 1999; Sullivan et al., 1994). The high sensitivity of NMDA receptors to reducing agents, compared with oxidizers, is thought to be the result of extracellular redox sites being maintained in a predominantly oxidized state because extracellular antioxidants are produced within the cell and are slow to diffuse out (Jones et al., 2000; Ottaviano et al., 2008). This may also explain why the effects of H_2O_2 were reversed by reperfusion but the effects of MPG and NAC were not, similar to other studies in which the effects of oxidizing but not reducing agents were reversed by washout (Bodhinathan et al., 2010; Köhr et al., 1994). Because cellular ROS production is slow, if extracellular levels are eliminated, it may take some time before baseline concentrations are re-established and scavenging agents are degraded (Ottaviano et al., 2008).

Blocking mitochondrial ROS production using the complex I inhibitor rotenone resulted in increases in NMDA receptor activity to a degree similar to that of ROS scavenging, demonstrating that changes in mitochondrial ROS production can directly modulate NMDA receptor activity. Full recovery from rotenone treatment was achieved within the reperfusion period, supporting the idea that the lack of recovery seen during ROS scavenging is the result of delays in oxidation/degradation of the scavenging agents used. NMDA receptors are highly expressed in the post-synaptic densities of excitatory synapses, as are mitochondria, which provide the necessary ATP for synaptic activities (Danysz and Parsons, 1998; Ly and Verstreken, 2006). H_2O_2 produced from these mitochondria can freely diffuse across the cellular membrane, or move through ion channels, in order to oxidize extracellular NMDA receptor redox modulatory sites (Mollajew et al., 2010; Ottaviano et al., 2008). The function of NMDA receptor redox control or the connection to the mitochondria has yet to be established; however, we propose that ROS changes may be involved in a negative feedback system between mitochondria, a primary site for intracellular Ca^{2+} storage/regulation, and NMDA receptor-mediated Ca^{2+} entry. Mitochondrial ROS generation is increased by NMDA receptor activation unless blocked by the removal of extracellular Ca^{2+}, mitochondrial uncouplers or Ca^{2+} uniporter inhibitors (Duan et al., 2007; Dugan et al., 1995). A feedback loop between Ca^{2+} influx and storage could be utilized to prevent excessive uptake leading to cell death.

The mechanism by which Ca^{2+} release from the mitochondria is triggered has yet to be established. We have proposed that it is the result of mK_{ATP} activation and subsequent formation of low-conductance mitochondrial permeability transition pores (mPTPs) (Pamenter et al., 2008a; Zivkovic and Buck, 2010; Hawrysh and Buck, 2013). mK_{ATP} channels remain closed under normoxic conditions when ATP levels are high and are activated during anoxia as mitochondrial ATP production decreases. Opening of the channel permits an influx of K^+ into the mitochondria that triggers mPTP formation and Ca^{2+} release (Murchison and Griffith, 2000). In the western painted turtle, addition of the mPTP activator atractyloside decreases NMDA receptor currents and increases $[Ca^{2+}]_i$ to levels comparable to those induced by anoxia, and the addition of the Ca^{2+} chelator BAPTA blocks the decrease in NMDA receptor currents (Hawrysh and Buck, 2013). The mechanism through which an increase in $[Ca^{2+}]_i$ brings about a decrease in NMDA and AMPA receptor currents has previously been attributed to increases in the activity of the Ca^{2+}-binding messenger protein calmodulin (Ca^{2+}/calmodulin) and subsequent activation of the Ca^{2+}/calmodulin-dependent phosphatase PP2B (calcineurin) (Shin et al., 2005). Calmodulin binding and dephosphorylation of NMDA receptor subunits during anoxia may cause changes in protein conformation that block/inhibit NMDA receptor redox sites and decrease NMDA receptor activity.

We have shown that decreases in $[ROS]_i$ increase NMDA receptor activity; however, receptor currents decrease during anoxia, which indicates that a secondary mechanism overrides modulatory redox control and initiates receptor inhibition. Replicating the anoxia-mediated increase in mitochondrial Ca^{2+} release with the mK_{ATP} channel agonist diazoxide produced a decrease in NMDA receptor currents comparable to anoxia and was unaffected by MPG application, indicating that Ca^{2+} release overrides redox control. It is important to note that application of diazoxide after MPG addition was not successful in reversing the large increases in NMDA receptor currents brought about by ROS scavenging, suggesting that if increases in $[Ca^{2+}]_i$ do not occur before ROS decreases, NMDA receptor activity will rise and may lead to ECD. This effect was also seen when the anoxia-mediated increase in $[Ca^{2+}]_i$ was blocked with a Ca^{2+} chelator, which prevented the anoxia-mediated downregulation of the NMDA receptor and also produced significant increases in NMDA receptor currents, potentially as a result of ROS decreases (Shin et al., 2005). For mitochondrial Ca^{2+} release to prevent redox-induced NMDA receptor potentiation activation of mK_{ATP} channels, mPTP formation and mitochondrial Ca^{2+} release must all occur before anoxic decreases in ROS. To assess the timing of intracellular anoxia-mediated signals, we compared changes in Ψ_m, $[Ca^{2+}]_i$ and $[ROS]_i$. The onset of the increase in fluorescence of both rhodamine-123 and Oregon Green dyes occurred at ~70 s after the switch to anoxia. Because rhodamine-123 has a response time in the seconds–minutes range (Plášek and Sigler, 1996) and Oregon Green in the millisecond range (Canepari and Mammano, 1999), it is likely that Ψ_m depolarizion occurred prior to Ca^{2+} release. This finding further supports the hypothesis that anoxia-mediated depolarization of Ψ_m is the signal to induce mitochondrial Ca^{2+} release. The onset of the anoxia-mediated Ca^{2+} signal occurs ~40 s before $[ROS]_i$ begin to decrease and reaches steady state ~400 s before $[ROS]_i$ reaches steady state. We propose that this provides sufficient time to inhibit NMDA receptors before redox modulation could occur. Interestingly, changes in Ψ_m and $[Ca^{2+}]_i$ occurred before the bath chamber $\dot{P}_{O_2}$ reached ~0 mmHg, indicating that depolarization of Ψ_m occurs before tissue $\dot{P}_{O_2}$ reaches 0 mmHg. When considering the aforementioned information collectively, we conclude that the time dependency of Ca^{2+} release is crucial with respect to changes in ROS, and this order of events may have been selected for in the turtle brain.

In summary, we have demonstrated that decreases in $[ROS]_i$ during anoxia within the cortical pyramidal neurons of the western painted turtle are not responsible for triggering downregulation of

NMDA and AMPA receptors. Instead, we have provided evidence that NMDA receptors in turtle pyramidal neurons respond to oxidative/reductive challenges in a manner similar to other vertebrate species. Our findings indicate that during the transition to anoxia, mitochondrial Ca^{2+} release prior to depletion of ROS levels is essential for overriding mechanisms of redox control and the downregulation NMDA and AMPA receptor activity.

MATERIALS AND METHODS

Animals

This study was approved by the University of Toronto Animal Care Committee and conforms to the relevant guidelines issued by the Canadian Council on Animal Care regarding the care and use of experimental animals. Adult female turtles (carapace length ~15 cm, 200–300 g) were purchased from Niles Biological Inc. (Sacramento, CA, USA). The animals were housed in large indoor ponds (2×4×1.5 m) equipped with a basking platform, heating lamp and a flow-through dechlorinated freshwater system. The water temperature was maintained at ~18°C and the air temperature at 20°C. Turtles were given continuous access to food and kept on a 12 h:12 h light:dark photoperiod.

Cortical brain sheet preparation and experimental setup

Basic protocols for cortical sheet dissection and whole-cell patch clamp recordings under normoxic and anoxic conditions are described elsewhere (Shin and Buck, 2003). Briefly, turtles were decapitated and the whole brain was rapidly excised from the cranium within 30 s of decapitation. Six cortical sheets were isolated from whole brains and bathed in artificial cerebrospinal fluid (aCSF; in mmol l^{-1}): 107 NaCl, 2.6 KCl, 1.2 $CaCl_2$, 1 $MgCl_2$, 2 $NaH_2PO_4 \cdot 2H_2O$, 26.5 $NaHCO_3$, 10 glucose and 5 imidazole (pH 7.4; osmolarity 285–290 mOsm). Cortical sheets were placed in an RC-26 chamber with a P1 platform (Warner Instruments, Hamden, CT, USA). The chamber was gravity perfused with aCSF at a rate of 2–3 ml min^{-1}. Normoxic aCSF was gassed with air/5% CO_2 and anoxic aCSF with 95% N_2/5% CO_2. Preliminary experiments comparing the use of 95% O_2/5% CO_2 and air/5% CO_2 demonstrated that there were no differences in any of the results and of particular note, switching between 95% O_2 and air had no effect on ROS production. To maintain anoxic conditions in the bathing chamber, perfusion tubes from the intravenous bottle were double jacketed and the outer jacket was gassed with 95% N_2/5% CO_2 and a plastic cover with a hole for the recording electrode was placed over the perfusion chamber, and the space between the fluid surface and cover was gently gassed with 95% N_2/5% CO_2. The anoxic aCSF reservoir was bubbled vigorously for 30 min prior to an experiment and gently throughout the experiment to maintain anoxic conditions. $\dot{P}_{O_2}$ in bath aCSF decreased to ~0 mmHg under these experimental conditions in ~10 min (i.e. bath $\dot{P}_{O_2}$ was not different from reservoir $\dot{P}_{O_2}$; see Results and Fig. 6A for timeline of $\dot{P}_{O_2}$ changes). Bath chamber $\dot{P}_{O_2}$ was measured using a fluorescent oxygen analyzer and Witrox-1 v1.6.0 software (Witrox 1, Loligo Systems, Denmark). A fast-step drug perfusion system (VC-6 model perfusion valve controller and SF-77B fast-step perfusion system; Warner Instruments) was used to deliver pharmacological modifiers directly above the cortical sheet (see details below). Fast-step perfusion syringes were also bubbled and jacketed in the same manner as above to maintain anoxic conditions. All experiments were performed at a room temperature of 22°C.

Whole-cell patch clamp electrophysiology

Whole-cell recordings from pyramidal neurons located in the dorsomedial area of the dorsal cortex were obtained using fire-polished 4–6 MΩ borosilicate glass pipettes (Harvard Apparatus LTD, Holliston, MA, USA). Pipette solutions contained (in mmol l^{-1}): 8 NaCl, 0.0001 $CaCl_2$, 10 Na HEPES, 110 K gluconate, 1 $MgCl_2$, 0.3 NaGTP and 2 NaATP (pH 7.4; osmolarity 295–300 mOsM). An Ag-AgCl electrode connected to a CV-7B headstage and MultiClamp 700B amplifier (Molecular Devices, Sunnyvale, CA, USA) was inserted into pipettes and a motorized patch-clamp micromanipulator (Burleigh, PCS-6000 series, Thorlabs, Newton, NJ, USA) was used to position them within the tissue. Cell-attached 5–10 GΩ seals were obtained using blind-patch techniques described elsewhere (Blanton et al., 1989). Upon seal formation, negative pressure was applied to achieve the whole-cell patch-clamp configuration. Following whole-cell capacitance compensation, typical whole-cell access resistance (R_a) was 20–25 MΩ. R_a was determined before each measurement and recordings were discarded if R_a changed by more than 20% or whole-cell leak currents changed by more than 30 pA during the course of the experiment. Prior to the commencement of experiments, a step protocol to identify cell type was performed as described elsewhere (Shin and Buck, 2003), and patches from non-pyramidal cells were discarded. All data were collected at 5–10 kHz using an Axopatch-1D amplifier, a CV-4 head stage and a Digidata 1200 interface, and analyzed using Clampex 10 software (Molecular Devices).

Evoked NMDA and AMPA receptor current recordings

Following membrane rupture and formation of the whole-cell patch, a 5 min period was allowed for patch stabilization prior to commencement of recordings. Control evoked NMDA/AMPA receptor currents were recorded at the start of the experiment at (t=0 min) and following 10 min of normoxic perfusion. The initial current recording was set to a value of 100% and all subsequent recordings were normalized to that first control value. The second control value (t=10 min) was used to confirm consistency within the normoxic recordings and for future statistical analysis. Cells were next perfused with experimental bulk aCSF treatments and/or drip perfusions. Experimental conditions were maintained for 40–80 min and evoked current recordings were taken at 20 min intervals. The tissue was reperfused following the experimental treatment period with control normoxic aCSF for 40 min and current recordings were taken at 20 min intervals.

Fluorescence measurements

In all fluorescence experiments, cortical sheets were placed in a flow-though bath chamber of an upright microscope (Olympus BX51WI) equipped with an Olympus 0.8 NA, 40× water immersion objective. Dyes were imaged using a FITC filter set (Semrock, Rochester, NY, USA) and a monochromonator (Photon Technology International, London, ON, Canada), controlled by Easy Ratio Pro imaging software (Photon Technology International). Fluorescence emissions were detected with an EMCCD camera (Rolera-MG*i*, Q Imaging, Burnaby, BC, Canada). Neurons were excited for 0.5 s every 10 s to prevent bleaching of the dye and permit experiments of up to an hour in length. To assess whether endogenous fluorescence of cortical sheets affects fluorescence measurements, control cortical sheets were exposed to each treatment in the absence of fluorophores. The background fluorescence was minimal and remained constant with each treatment; therefore, background fluorescence was not subtracted from fluorescent data. For statistical analysis, 10 neurons per cortical sheet were chosen at random and the average change in regions of interest from the center of the cell body was used as a single replicate. Brightly fluorescing cells were avoided. Sample traces were smoothed using Easy Ratio Pro imaging software to reduce noise and simplify interpretation. Oregon Green and rhodamine traces were drift corrected to a linear regression line fit to the 10 min normoxic portion of the trace to enable comparison and produce average traces (Fig. 6).

CM-DCF fluorescence measurements for $[ROS]_i$

Changes in $[ROS]_i$ were assessed using the membrane-permeable ROS-sensitive fluorescent indicator 5-(and-6)-chloromethyl-2′,7′-dichlorodihydrofluorescein diacetate, acetyl ester (CM-H_2DCFDA; Invitrogen, Burlington, ON, Canada). Cortical sheets were incubated in aCSF containing 5 μmol l^{-1} CM-H_2DCFDA (from a 1 mmol l^{-1} stock solution in DMSO) for 30 min (4°C) followed by a 30 min wash in aCSF (22°C). During loading, the acetate groups on CM-H_2DCFDA are removed by intracellular esterases, preventing dye leakage. Steady-state normoxic generation of ROS results in oxidation of the CM-H_2DCF to CM-DCF and a subsequent increase in fluorescence. CM-DCF was excited with a wavelength of 495 nm and fluorescence emission was detected at wavelength of 520 nm. Cortical sheets were exposed to treatment aCSF for 30 min then reperfused with control aCSF for 20 min or treated with 50 μmol l^{-1} H_2O_2 for 5 min. Cessation of ROS generation results in no change in CM-DCF fluorescence. To assess treatment effects on ROS generation, the fluorescence at treatment steady state was compared with a

linear regression line fit to the 10 min normoxic portion of the trace. Data are presented as percent change expressed relative to that fitted normoxic regression line (Crowe et al., 1995).

Oregon Green fluorescence measurements for $[Ca^{2+}]_i$

Changes in $[Ca^{2+}]_i$ were assessed using the membrane-permeable Ca^{2+}-sensitive fluorescent indicator Oregon Green 488 BAPTA-1 AM (Invitrogen). Oregon Green was selected because of its high Ca^{2+} affinity (K_d≈170 nmol l^{-1}) and previous use in turtle cortical tissue (Hawrysh and Buck, 2013). Cortical sheets were incubated in aCSF containing 5 µmol l^{-1} Oregon Green (from a 1 mmol l^{-1} stock solution in DMSO) for two consecutive 1 h periods at 4°C followed by a 30 min wash in aCSF (22°C). The double loading period resulted in elevated baseline fluorescence levels, indicating sufficient dye uptake. Oregon Green was excited with a wavelength of 488 nm and fluorescence emissions were detected at a wavelength of 520 nm. Cortical sheets were exposed to treatment aCSF for 20–40 min then reperfused with control aCSF for at least 10 min to allow fluorescence to return to baseline. Once each experiment was completed, aCSF flow was halted and tissues were incubated in ionomycin (2 µmol) for 5 min, followed by application of $MnCl_2$ (2 mmol l^{-1}), to quench the Ca^{2+} fluorescence signal and obtain a value for background fluorescence. This value was subtracted from all recordings during analysis to isolate the fluorescence attributed to changes in $[Ca^{2+}]$. The protocol and concentrations used were based on previous investigations (Hawrysh and Buck, 2013).

Rhodamine-123 fluorescence measurements for mitochondrial membrane potential (Ψ_m)

Cortical neurons were loaded with the membrane-permeable Ψ_m-sensitive dye rhodamine-123 (Invitrogen) for 50 min (4°C). Rhodamine-123 was dissolved in DMSO to a stock concentration of 25 mmol l^{-1} and then diluted to 50 µmol l^{-1} in aCSF. Following dye loading, cortical sheets were washed in aCSF (22°C) for 20 min. Rhodamine-123 was excited at a wavelength of 495 nm and fluorescence emissions were detected at a wavelength of 520 nm. Cortical sheets were exposed to treatment aCSF for 30 min and then reperfused with control aCSF for 30 min to allow fluorescence to return to baseline. The protocol and concentrations used were based on previous investigations (Hawrysh and Buck, 2013).

Pharmacology and drug administration

Decreases in $[ROS]_i$ was achieved through the separate application of two cell-permeable ROS scavengers: MPG (0.5 mmol l^{-1}) and NAC (0.5 mmol l^{-1}). Direct increases in ROS were induced through drip application of cell-permeable H_2O_2 (50 µmol l^{-1}) as it represented the primary mitochondrial ROS product (Chen et al., 2003; Ottaviano et al., 2008). Mitochondrial-specific ROS production was halted using the complex I inhibitor rotenone (25 µmol l^{-1}). Rotenone has been successfully used in other vertebrate tissues to decrease $[ROS]_i$ (Li and Trush, 1998; Liu et al., 2002; Liu et al., 1993). $[Ca^{2+}]_i$ increases were replicated using the mK_{ATP} channel agonist diazoxide (100 µmol l^{-1}). Diazoxide is a potent activator of mK_{ATP} channels as demonstrated by K^+ flux in bovine heart mitochondria, which possess a 1000-fold greater sensitivity to diazoxide than the sarcolemma (Garlid et al., 1997). Furthermore, diazoxide application to turtle cortical neurons results in a depolarization of Ψ_m, release of mitochondrial $[Ca^{2+}]$, and a decrease in NMDA/AMPA receptor currents to levels comparable to those seen during anoxia (Hawrysh and Buck, 2013; Pamenter et al., 2008a; Zivkovic and Buck, 2010). Concentrations of rotenone and diazoxide were based on previous experiments on turtle cortical tissue (Pamenter et al., 2007). Diazoxide was initially solubilized in DMSO (1% in final solution) and rotenone was solubilized in chloroform before being diluted further in aCSF (0.05% in final solution). DMSO was not utilized to dissolve rotenone as the combination often caused the solution to become cloudy. All other pharmacological compounds were dissolved in aCSF. During whole-cell recordings, both ROS scavengers and rotenone were drip and bulk perfused. Diazoxide and H_2O_2 were administered through drip application only. In addition, H_2O_2 was administered for only 5 min prior to tetrodotoxin administration in order to limit potential toxicity. For experiments involving Ca^{2+} chelation, BAPTA (5 mmol l^{-1}) was included in the recording electrode solution. Tetrodotoxin was purchased from Tocris Bioscience (Ellisville, MO, USA) and all other chemicals were obtained from Sigma-Aldrich (Oakville, ON, Canada).

Statistical analysis

Data were analyzed using SigmaPlot software version 11.0 (Systat Software, Inc., San Jose, CA, USA). Fluorescence and $\dot{P}_{O_2}$ data were analyzed by one-way ANOVA followed by a Tukey's *post hoc* test to identify differences between treatment and control groups. NMDA and AMPA receptor whole-cell peak current amplitude data were analyzed using a one-way repeated-measures ANOVA. Data were divided by 1000 and arcsine transformed to normally distribute the data prior to statistical analysis. An ANOVA was used to compare the means of normoxic controls and treatments within treatment groups. Significance for all data was determined at $P<0.05$. Results are expressed as means ± s.e.m.

Acknowledgements

The authors thank Aaron Chowdhury for assistance with fiber-optic oxygen measurements in the tissue recording chamber and saline reservoirs.

Competing interests

The authors declare no competing financial interests.

Author contributions

L.T.B. and D.J.D. conceived and designed the study. D.J.D., D.W.H. and P.J.H. performed the experiments and analysed the data. D.J.D. wrote the first draft of the manuscript. L.T.B. and D.W.H. revised and prepared the final version of the manuscript for publication.

Funding

Research funding was provided by the Natural Sciences and Engineering Research Council of Canada to L.T.B.

References

Aizenman, E., Lipton, S. A. and Loring, R. H. (1989). Selective modulation of NMDA responses by reduction and oxidation. *Neuron* **2**, 1257-1263.
Bickler, P. E. (1998). Reduction of NMDA receptor activity in cerebrocortex of turtles (*Chrysemys picta*) during 6 wk of anoxia. *Am. J. Physiol.* **275**, R86-R91.
Blanton, M. G., Lo Turco, J. J. and Kriegstein, A. R. (1989). Whole cell recording from neurons in slices of reptilian and mammalian cerebral cortex. *J. Neurosci. Methods* **30**, 203-210.
Bodhinathan, K., Kumar, A. and Foster, T. C. (2010). Intracellular redox state alters NMDA receptor response during aging through Ca2+/calmodulin-dependent protein kinase II. *J. Neurosci.* **30**, 1914-1924.
Bosley, T. M., Woodhams, P. L., Gordon, R. D. and Balázs, R. (1983). Effects of anoxia on the stimulated release of amino acid neurotransmitters in the cerebellum *in vitro*. *J. Neurochem.* **40**, 189-201.
Canepari, M. and Mammano, F. (1999). Imaging neuronal calcium fluorescence at high spatio-temporal resolution. *J. Neurosci. Methods* **87**, 1-11.
Chandel, N. S. and Schumacker, P. T. (2000). Cellular oxygen sensing by mitochondria: old questions, new insight. *J. Appl. Physiol.* **88**, 1880-1889.
Chen, Q., Vazquez, E. J., Moghaddas, S., Hoppel, C. L. and Lesnefsky, E. J. (2003). Production of reactive oxygen species by mitochondria: central role of complex III. *J. Biol. Chem.* **278**, 36027-36031.
Choi, D. W. (1992). Excitotoxic cell death. *J. Neurobiol.* **23**, 1261-1276.
Choi, Y. B. and Lipton, S. A. (2000). Redox modulation of the NMDA receptor. *Cell. Mol. Life Sci.* **57**, 1535-1541.
Choi, Y., Chen, H. V. and Lipton, S. A. (2001). Three pairs of cysteine residues mediate both redox and zn2+ modulation of the nmda receptor. *J. Neurosci.* **21**, 392-400.
Cross, J. V. and Templeton, D. J. (2006). Regulation of signal transduction through protein cysteine oxidation. *Antioxid. Redox Signal.* **8**, 1819-1827.
Crowe, W. E., Altamirano, J., Huerto, L. and Alvarez-Leefmans, F. J. (1995). Volume changes in single N1E-115 neuroblastoma cells measured with a fluorescent probe. *Neuroscience* **69**, 283-296.
D'Autréaux, B. and Toledano, M. B. (2007). ROS as signalling molecules: mechanisms that generate specificity in ROS homeostasis. *Nat. Rev. Mol. Cell Biol.* **8**, 813-824.
Danysz, W. and Parsons, C. G. (1998). Glycine and *N*-methyl-D-aspartate receptors: physiological significance and possible therapeutic applications. *Pharmacol. Rev.* **50**, 597-664.
Duan, Y., Gross, R. A. and Sheu, S.-S. (2007). Ca^{2+}-dependent generation of mitochondrial reactive oxygen species serves as a signal for poly(ADP-ribose) polymerase-1 activation during glutamate excitotoxicity. *J. Physiol.* **585**, 741-758.
Dugan, L. L., Sensi, S. L., Canzoniero, L. M., Handran, S. D., Rothman, S. M., Lin, T. S., Goldberg, M. P. and Choi, D. W. (1995). Mitochondrial production of reactive oxygen species in cortical neurons following exposure to *N*-methyl-D-aspartate. *J. Neurosci.* **15**, 6377-6388.
Garlid, K. D., Paucek, P., Yarov-Yarovoy, V., Murray, H. N., Darbenzio, R. B., D'Alonzo, A. J., Lodge, N. J., Smith, M. A. and Grover, G. J. (1997).

Cardioprotective effect of diazoxide and its interaction with mitochondrial ATP-sensitive K^+ channels. Possible mechanism of cardioprotection. *Circ. Res.* **81**, 1072-1082.

Gozlan, H. and Ben-Ari, Y. (1995). NMDA receptor redox sites: are they targets for selective neuronal protection? *Trends Pharmacol. Sci.* **16**, 368-374.

Gozlan, H., Khazipov, R., Diabira, D. and Ben-Ari, Y. (1995). In CA1 hippocampal neurons, the redox state of NMDA receptors determines LTP expressed by NMDA but not by AMPA receptors. *J. Neurophysiol.* **73**, 2612-2617.

Hawrysh, P. J. and Buck, L. T. (2013). Anoxia-mediated calcium release through the mitochondrial permeability transition pore silences NMDA receptor currents in turtle neurons. *J. Exp. Biol.* **216**, 4375-4387.

Henzler, T. and Steudle, E. (2000). Transport and metabolic degradation of hydrogen peroxide in *Chara corallina*: model calculations and measurements with the pressure probe suggest transport of H_2O_2 across water channels. *J. Exp. Bot.* **51**, 2053-2066.

Hoyt, K. R., Gallagher, A. J., Hastings, T. G. and Reynolds, I. J. (1997). Characterization of hydrogen peroxide toxicity in cultured rat forebrain neurons. *Neurochem. Res.* **22**, 333-340.

Jackson, D. C. (2000). Living without oxygen: lessons from the freshwater turtle. *Comp. Biochem. Physiol.* **125A**, 299-315.

Jackson, D. C. and Ultsch, G. R. (1982). Long-term submergence at 3°C of the turtle, *Chrysemys picta bellii*, in normoxic and severely hypoxic water. 2. Extracellular ionic responses to extreme lactic-acidosis. *J. Exp. Biol.* **96**, 29-43.

Janáky, R., Varga, V., Saransaari, P. and Oja, S. S. (1993). Glutathione modulates the *N*-methyl-D-aspartate receptor-activated calcium influx into cultured rat cerebellar granule cells. *Neurosci. Lett.* **156**, 153-157.

Jones, D. P., Carlson, J. L., Mody, V. C., Jr, Cai, J., Lynn, M. J. and Sternberg, P., Jr (2000). Redox state of glutathione in human plasma. *Free Radic. Biol. Med.* **28**, 625-635.

Kim, W.-K., Choi, Y.-B., Rayudu, P. V., Das, P., Asaad, W., Arnelle, D. R., Stamler, J. S. and Lipton, S. A. (1999). Attenuation of NMDA receptor activity and neurotoxicity by nitroxyl anion, NO^-. *Neuron* **24**, 461-469.

Köhr, G., Eckardt, S., Lüddens, H., Monyer, H. and Seeburg, P. H. (1994). NMDA receptor channels: subunit-specific potentiation by reducing agents. *Neuron* **12**, 1031-1040.

Lei, B., Adachi, N. and Arai, T. (1998). Measurement of the extracellular H_2O_2 in the brain by microdialysis. *Brain Research Protocols* **3**, 33-36.

Li, Y. and Trush, M. A. (1998). Diphenyleneiodonium, an NAD(P)H oxidase inhibitor, also potently inhibits mitochondrial reactive oxygen species production. *Biochem. Biophys. Res. Commun.* **253**, 295-299.

Liu, Y., Rosenthal, R. E. and Fiskum, G. (1993). H_2O_2 release by isolated brain mitochondria in a canine cerebral ischemia/reperfusion model. *FASEB J.* **7**, A424.

Liu, Y., Fiskum, G. and Schubert, D. (2002). Generation of reactive oxygen species by the mitochondrial electron transport chain. *J. Neurochem.* **80**, 780-787.

Ly, C. V. and Verstreken, P. (2006). Mitochondria at the synapse. *Neuroscientist* **12**, 291-299.

Milton, S. L., Nayak, G., Kesaraju, S., Kara, L. and Prentice, H. M. (2007). Suppression of reactive oxygen species production enhances neuronal survival *in vitro* and *in vivo* in the anoxia-tolerant turtle *Trachemys scripta*. *J. Neurochem.* **101**, 993-1001.

Mollajew, R., Zocher, F., Horner, A., Wiesner, B., Klussmann, E. and Pohl, P. (2010). Routes of epithelial water flow: aquaporins versus cotransporters. *Biophys. J.* **99**, 3647-3656.

Murchison, D. and Griffith, W. H. (2000). Mitochondria buffer non-toxic calcium loads and release calcium through the mitochondrial permeability transition pore and sodium/calcium exchanger in rat basal forebrain neurons. *Brain Res.* **854**, 139-151.

Nilsson, G. E. and Lutz, P. L. (1991). Release of inhibitory neurotransmitters in response to anoxia in turtle brain. *Am. J. Physiol.* **261**, R32-R37.

Ottaviano, F. G., Handy, D. E. and Loscalzo, J. (2008). Redox regulation in the extracellular environment. *Circ. J.* **72**, 1-16.

Pamenter, M. E., Richards, M. D. and Buck, L. T. (2007). Anoxia-induced changes in reactive oxygen species and cyclic nucleotides in the painted turtle. *J. Comp. Physiol. B* **177**, 473-481.

Pamenter, M. E., Shin, D. S.-H., Cooray, M. and Buck, L. T. (2008a). Mitochondrial ATP-sensitive K^+ channels regulate NMDAR activity in the cortex of the anoxic western painted turtle. *J. Physiol.* **586**, 1043-1058.

Pamenter, M. E., Shin, D. S. H. and Buck, L. T. (2008b). AMPA receptors undergo channel arrest in the anoxic turtle cortex. *Am. J. Physiol.* **294**, R606-R613.

Pamenter, M. E., Hogg, D. W., Ormond, J., Shin, D. S., Woodin, M. A. and Buck, L. T. (2011). Endogenous $GABA_A$ and $GABA_B$ receptor-mediated electrical suppression is critical to neuronal anoxia tolerance. *Proc. Natl. Acad. Sci.* **108**, 11274-11279.

Pérez-Pinzón, M. A., Chan, C. Y., Rosenthal, M. and Sick, T. J. (1992). Membrane and synaptic activity during anoxia in the isolated turtle cerebellum. *Am. J. Physiol.* **263**, R1057-R1063.

Plášek, J. and Sigler, K. (1996). Slow fluorescent indicators of membrane potential: a survey of different approaches to probe response analysis. *J. Photochem. Photobiol. B* **33**, 101-124.

Rhee, S. G., Chang, T.-S., Bae, Y. S., Lee, S.-R. and Kang, S. W. (2003). Cellular regulation by hydrogen peroxide. *J. Am. Soc. Nephrol.* **14 Suppl. 3**, S211-S215.

Shin, D. S.-H. and Buck, L. T. (2003). Effect of anoxia and pharmacological anoxia on whole-cell NMDA receptor currents in cortical neurons from the western painted turtle. *Physiol. Biochem. Zool.* **76**, 41-51.

Shin, D. S.-H., Wilkie, M. P., Pamenter, M. E. and Buck, L. T. (2005). Calcium and protein phosphatase 1/2A attenuate *N*-methyl-D-aspartate receptor activity in the anoxic turtle cortex. *Comp. Biochem. Physiol.* **142A**, 50-57.

Sies, H. (1993). Strategies of antioxidant defense. *Eur. J. Biochem.* **215**, 213-219.

Starkov, A. A. (2008). The role of mitochondria in reactive oxygen species metabolism and signaling. *Ann. N. Y. Acad. Sci.* **1147**, 37-52.

Sullivan, J. M., Traynelis, S. F., Chen, H.-S. V., Escobar, W., Heinemann, S. F. and Lipton, S. A. (1994). Identification of two cysteine residues that are required for redox modulation of the NMDA subtype of glutamate receptor. *Neuron* **13**, 929-936.

Ulinski, P. S. (2007). Visual cortex of turtles. In *Evolution of Nervous Systems*, Vol. 2 (ed. J. H. Kaas), pp. 195-203. London: Elsevier.

Zivkovic, G. and Buck, L. T. (2010). Regulation of AMPA receptor currents by mitochondrial ATP-sensitive K+ channels in anoxic turtle neurons. *J. Neurophysiol.* **104**, 1913-1922.